P H Y S I C A L   R E V I E W   L E T T E R S

Observation and Control of Shock Waves in Individual Nanoplasmas

Daniel D. Hickstein,[1] Franklin Dollar,[1] Jim A. Gaffney,[2] Mark E. Foord,[2] George M. Petrov,[3] Brett B. Palm,[4] K. Ellen Keister,[1] Jennifer L. Ellis,[1] Chengyuan Ding,[1] Stephen B. Libby,[2] Jose L. Jimenez,[4] Henry C. Kapteyn,[1] Margaret M. Murnane,[1] and Wei Xiong[1]

[1]*Department of Physics, University of Colorado and JILA, National Institute of Standards and Technology and University of Colorado, Boulder, Colorado 80309, USA*
[2]*Physics Division, Physical and Life Sciences, Lawrence Livermore National Laboratory, Livermore, California 94550, USA*
[3]*Plasma Physics Division, Naval Research Lab, Washington, District of Columbia 20375, USA*
[4]*Department of Chemistry and Biochemistry and CIRES, University of Colorado, Boulder, Colorado 80309, USA*

Using an apparatus that images the momentum distribution of individual, isolated 100-nm-scale plasmas, we make the first experimental observation of shock waves in nanoplasmas. We demonstrate that the introduction of a heating pulse prior to the main laser pulse increases the intensity of the shock wave, producing a strong burst of quasimonoenergetic ions with an energy spread of less than 15%. Numerical hydrodynamic calculations confirm the appearance of accelerating shock waves and provide a mechanism for the generation and control of these shock waves. This observation of distinct shock waves in dense plasmas enables the control, study, and exploitation of nanoscale shock phenomena with tabletop-scale lasers.

Nanoscale plasmas (nanoplasmas) offer enhanced laser absorption compared to solid or gas targets [1], enabling high-energy physics with tabletop-scale lasers. Indeed, previous experimental studies have observed the production of high-energy ions [2] and even nuclear fusion [3] in laser-irradiated nanoplasmas. For more than a decade, theoretical studies have predicted that shock waves can be generated in nanoplasmas and that these nanoplasma shock waves might allow for the practical generation of quasimonoenergetic high-energy ions, neutrons from fusion processes, or ultrafast x-ray bursts [4–6].

An analytical study by Kaplan *et al.* suggests that shocks should be a common phenomenon in expanding nanoplasmas, requiring only a plasma density distribution that is highest in the center and decays smoothly towards the edges [5]. Similarly, Peano *et al.* [6,7] used numerical simulations to show that the density profile of the precursor nanoplasma would dictate the properties of the shock. In particular, they demonstrated that a weak laser pulse could be used to shape the density profile to so that a second, stronger laser pulse could produce more intense shock waves.

In contrast to the theoretical studies, which model a single nanoplasma, previous experimental studies of nanoplasmas [2,8] used laser focal volumes that contained many particles, thereby simultaneously irradiating nanoparticles of different sizes and with different laser intensities. As we show in this work, the kinetic energy of the shock wave depends on the plasma size and the laser intensity. Thus, studies that probe many nanoparticles simultaneously would create an ensemble of shock waves with different kinetic energies, thereby obscuring their identification as shocks.

In this Letter, by imaging individual laser-irradiated nanoparticles, we remove the size and intensity averaging present in previous studies, which allows us to clearly observe nanoscale plasma shock waves. Furthermore, we demonstrate that these shock waves can be controlled by using a laser pulse to shape the plasma density profile. Finally, we present hydrodynamic simulations that provide a mechanism for the generation and control of shock waves in nanoplasma.

Our observation of shock waves in nanoplasma is enabled by an experimental apparatus (Fig. 1) that can detect photoions from the nanoplasma generated from a single laser-irradiated nanoparticle. Nanocrystals of NaCl, KCl, KI, or NH_4NO_3 with diameters of ∼100 nm are created using a compressed-gas atomizer and introduced into the vacuum chamber using an aerodynamic lens. A plasma is formed via illumination of a particle with a tightly focused 40-fs laser pulse (wavelength of either 400 or 800 nm) with an intensity that is adjusted between 3×10^{13} and 4×10^{14} W/cm^2. The angle-resolved energy distribution of the ions created by the expanding nanoplasma is recorded using a velocity-map-imaging (VMI) photoion spectrometer [9–12] that records a two-dimensional projection of the photoion angular distribution (PAD).

Because the laser focal spot is small compared to the spacing between the nanoparticles, we probe, on average, one nanoplasma for every 40 laser shots (see the Supplemental Material [13] for complete experimental details). In all laser-irradiated nanoparticle experiments, each nanoparticle will experience a different laser intensity depending on where it is located in the laser focus, which
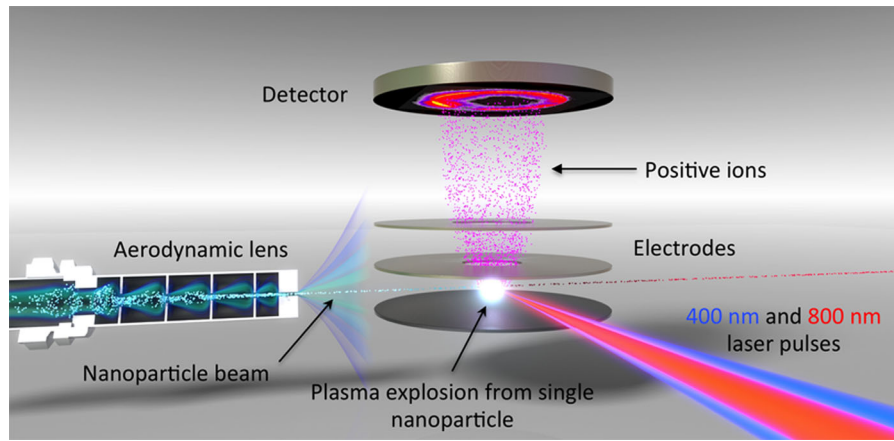
FIG. 1 (color online).   The apparatus for imaging shock waves in individual nanoplasmas. An aerodynamic lens focuses nanoparticles into a high-vacuum chamber where they are irradiated by a series of two time-delayed laser pulses. The first pulse creates an expanding nanoplasma, while the second pulse further heats the plasma, causing a pressure increase, which leads to shock wave formation. The resulting photoion momentum distribution is projected onto a microchannel-plate detector using three electrodes in a velocity-map-imaging geometry [12].

leads to intensity averaging effects if each PAD contains ions from many nanoparticles, as was the case in previous nanoplasma studies [14–16]. However, in this experiment, each PAD corresponds to a single particle and, although the intensity cannot be precisely controlled for each particle, no intensity averaging takes place within a single PAD. This allows for the observation of previously undiscovered physical processes, even those that are exquisitely sensitive to laser intensity, particle size, or particle composition.

In our experiment, when the peak laser intensity is below 5×10^{13} W/cm^2, the PADs contain only 100 or fewer ions, corresponding to the ionization of the residual N_2 and H_2O gas that flows with the particles through the aerodynamic lens. However, when the laser intensity is increased above $\sim 5 \times 10^{13}$ W/cm^2, we observe some PADs that contain more than 10^4 ions, indicating plasma formation in a single nanoparticle (Fig. S1) [13]. Indeed, in this intensity regime, solid nanoparticles are rapidly (<1 ps) converted into dense nanoplasmas through the following mechanism [16–18]. First, the strong laser field causes some of the atoms to ionize through tunnel ionization [8], liberating about one electron per atom within a few tens of femtoseconds [19]. These free electrons are accelerated by the strong laser field and then drive further rapid ionization through electron impact ionization [16]. The electrons continue to be driven by the laser field and absorb energy through collisions with the ions [20], reaching high temperatures.

When the laser intensity is increased above 1×10^{14} W/cm^2, shock waves appear in approximately 10% of the nanoparticle PADs (Figs. 2, S1, and S3). Each shock wave manifests as a sharp ridge on top of a broad photoion distribution. The ion kinetic energy of each shock ranges from 15 to 50 eV/Z, where Z is the charge state of the positive ion. However, each individual shock is
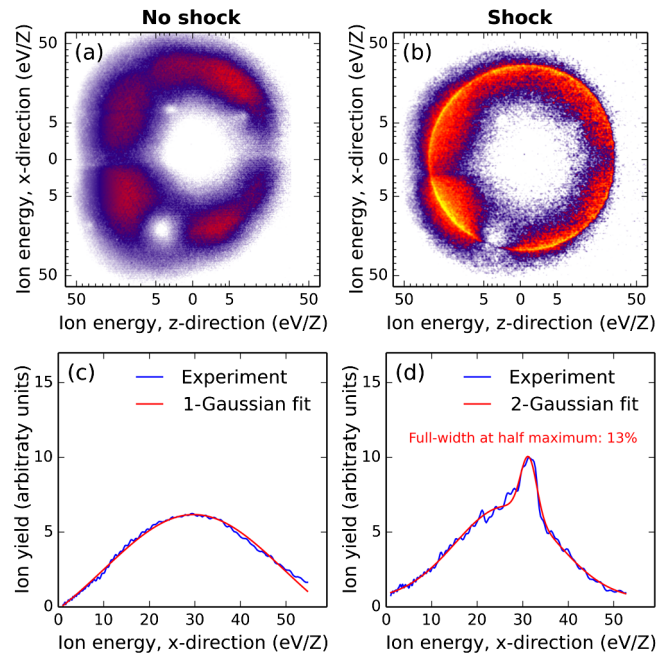

FIG. 2 (color online).   Observation of a shock wave from an individual nanoplasma. (a) The PAD from a single NH_4NO_3 nanoparticle irradiated with a pulse of 400-nm light followed by pulse of 800-nm light typically displays a broad ion distribution. Here, the laser propagates in the z direction (right to left) and is linearly polarized in the x direction. The angular features are due to the inhomogeneous responsivity of the imaging detector. (b) If the particle size, laser intensity, and laser pulse time delay are tuned appropriately, a sharp shock wave (orange and yellow regions) appears in addition to the broad ion distribution. (c) The radial energy distribution of the typical nanoplasma explosion can be fit by a single broad Gaussian function. (d) The shock wave manifests as an additional sharp peak, which can be fit by a second, narrower Gaussian function.

quasimonoenergetic, with an energy spread of less than
15% [Fig. 2(b)].

The formation of the shock waves is sensitive to both the
physical size and chemical composition of the particle.
We observe that larger nanoparticles are more likely to
create shock waves (Fig. S2), which can be explained by
the fact that larger nanoplasmas absorb more energy from
the laser field [1]. Using a single laser pulse, shocks are
observed in a variety of compounds, including KI, NaCl,
and KCl, and the threshold laser intensity required to create
shocks scales roughly with the ionization potential of the
compounds (Fig. S3), as expected for the onset of tunnel
ionization [19], and in agreement with the relative ioniza-
tion yields observed in single-particle mass spectroscopy
experiments [21]. For NH_4NO_3, the compound with the
highest ionization potential in this study, no shocks are
observed in the single-pulse experiment (Fig. S2), making
it the ideal example case for demonstrating the two-pulse
shock generation scheme.

Two laser pulses with an appropriate relative time delay
can be used to create shock waves in *all* of the materials
investigated in this study, including NH_4NO_3. The like-
lihood of shock formation depends critically on the time
delay between the first and second pulses. The minimum
time delay for shock creation coincides with the peak in the
total photoion yield, which occurs around 7 ps [Fig. 3(a)].
Similarly, the maximum time delay for shock production
occurs near 45 ps, corresponding to the end of the enhanced
ion yield. Previous studies [15,22] observed a similar
dependence of the photoion yield on time delay during
the two-pulse irradiation of nanoparticles (although they
did not observe shocks) and attributed this behavior to the
increased absorption of the second laser pulse caused
by the expansion of the plasma following the first
laser pulse.

The expansion of our nanoplasma into the vacuum is
significantly slower than previous studies due to the large
size of the nanoparticles and can be estimated using the ion
sound speed [8] $v_{expand} \approx \sqrt{ZkT_e/m_i}$, where Z is the
charge of the ions, m_i is the mass of the ions, and kT_e
is the electron temperature of the plasma. For N^{+1} with a
temperature of 10 eV, a 100-nm-diameter particle would
double in size in 6 ps, in good agreement with the 7-ps
delay for shock wave formation.

After the nanoparticle is irradiated by the first laser pulse,
the resulting plasma expands, and its density assumes a
radial profile that decays smoothly into vacuum. Energy
absorption peaks when the electron density of the plasma is
near the critical density [8,23], the density at which
electrons in the plasma are driven resonantly by the laser
field. As the plasma expands, the volume of plasma near the
critical density expands, enhancing energy absorption.
Eventually, the entire nanoplasma drops below the critical
density and light absorption is diminished. Thus, the arrival
time of the second pulse relative to the first determines the
amount of energy absorbed. The similarity of the time scale
for ion yield enhancement and the time scale for shock
formation suggests that the two effects share a common
mechanism: the expansion of the plasma between the first
and second pulses is crucial for the formation of shocks in
the two-pulse experiment.

The time delay between the laser pulses not only
determines the presence of shocks but also determines
the fraction of ions that become part of the shock wave. The
shocks produced with time delays of ∼10 ps involve a
small fraction of the ions, while the shocks generated using
time delays of >15 ps contain a much larger fraction of the
total ions [Figs. 3(b) and S4]. This indicates that the first
pulse is shaping the plasma density to achieve a density
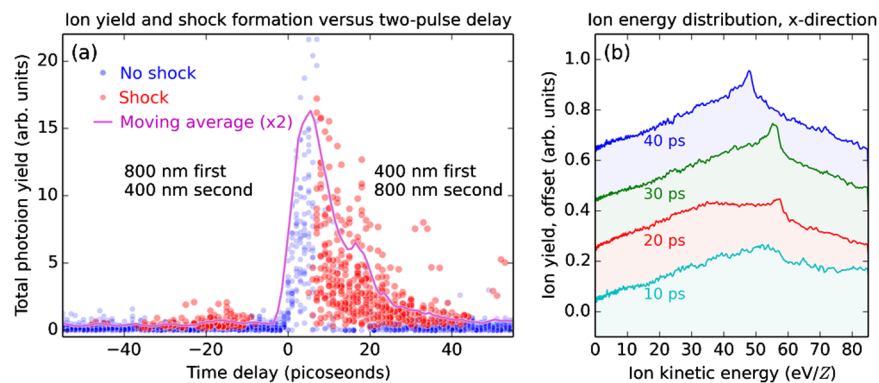profile that is better optimized for shock wave propagation

FIG. 3 (color online).   Control of shock wave formation using two laser pulses. (a) Each dot indicates a single nanoplasma explosion of
an individual NH_4NO_3 nanoparticle as a function of the delay between the 400- and 800-nm laser pulses. The first pulse forms a slowly
expanding nanoplasma, and the second pulse causes a rapid pressure increase inside of the nanoplasma, which leads to the formation of a
shock wave. When the delay between the two pulses is greater than 7 ps, shock waves are formed. The ion yield is higher when the
400-nm pulse precedes the 800-nm pulse because the 800-nm pulse is more effective at heating the expanded nanoplasma. (b) As the
relative time delay between the laser pulses is increased, the shocks become more pronounced. For comparison purposes, we display
shocks with energies ∼50 eV, although the shocks from different nanoparticles range between ∼15 and 50 eV/Z.
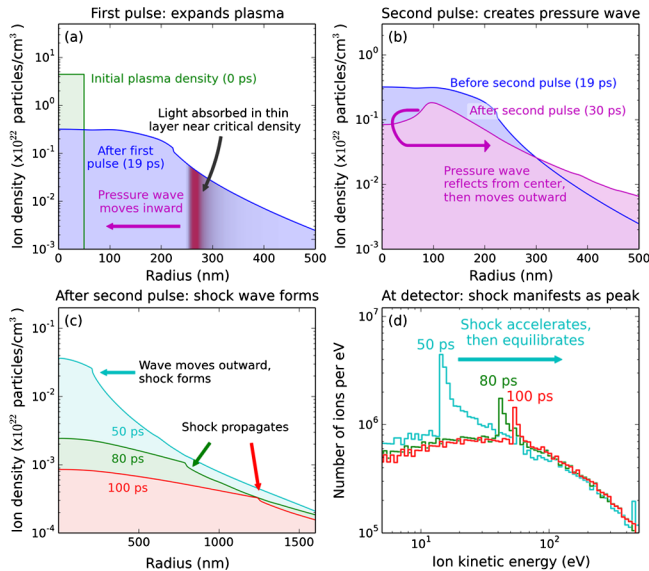
FIG. 4 (color online). The mechanism for two-pulse shock wave formation, as revealed by numerical hydrodynamics simulations using HYDRA [24]. (a) The first laser pulse creates a plasma, which expands into the surrounding vacuum. A small single-pulse shock wave can be seen near 230 nm. Near ~ 270 nm, energy from the second laser pulse is preferentially absorbed (red band) in a layer just below the critical density ($n_c \approx 1.7 \times 10^{21}$ at 800 nm). (b) The heating from the second laser pulse creates a pressure wave that moves inwards, reflects from the center, and then moves outwards. (c) The pressure wave moves outwards supersonically and accelerates slower material in front of it, creating a shock wave, which is seen as a small step in the ion density distribution. (d) In the kinetic energy distribution of the ions, the shock wave is a sharp peak which is accelerated by the pressure gradient, eventually settling at a final kinetic energy of a few tens of electron volts after ~ 100 ps. It is this asymptotic kinetic energy distribution that is recorded by the spectrometer in the experiment. In this simulation, both laser pulses are modeled as 50-fs, 800-nm pulses with intensities of 4.9×10^{14} W/cm^2.

and generation of quasimonoenergetic ions. Thus, this demonstrates that it is possible to control shock waves in plasmas by actively sculpting the plasma density profile using a femtosecond laser pulse.

To investigate the mechanism for shock formation, we employ numerical hydrodynamic simulations using the radiation hydrodynamics code HYDRA [24]. Details about the simulations are described in the Supplemental Material [13]. We simulate the interaction of two time-delayed laser pulses (each with an intensity of 4.9×10^{14} W/cm^2) with a 100-nm-diameter nanoparticle composed of NaCl. A prominent shock wave is observed for time delays between 5 and 35 ps (Figs. 4 and S5). In addition, the hydrodynamic simulations accurately reproduce measured ion kinetic energies. The good agreement between simulated and observed ion energies indicates that the hydrodynamic calculations capture the physics of the plasma expansion.

The hydrodynamic calculations suggest a simple mechanism for shock formation (Fig 4). After the first pulse expands the cluster, the second laser pulse is absorbed in a relatively thin shell at the critical density [Fig. 4(a)]. The resultant heating produces a large pressure increase in that region that drives material away from the absorption region [Fig. 4(b)]. This pressure wave reflects from the center of the plasma, resulting in a population of high-velocity ions at a small radius [Fig. 4(b)]. These ions drive an outward-moving shock [Fig. 4(c)], and the associated density increase produces a peak in the ion kinetic energy distribution [Fig. 4(d)]. The energy of the shock is determined both by the energy imparted by the laser and the work required for the high-velocity ions to accelerate the material ahead of them as they move to a large radius. Similar to previous theoretical predictions [4,5,25] of shock formation in the Coulomb explosion of small clusters, the shock formation occurs when faster particles towards the interior of the plasma overrun slower particles in the exterior of the cluster. However, in this case, the velocity differential is caused by the preferential absorption of light near the critical density, which creates a ridge of high pressure. In contrast to studies conducted in the Coulomb explosion regime, where the shock is formed on the time scale of 100 fs, the shocks in these hydrodynamic explosions take ~ 50 ps to form.

Interestingly, the hydrodynamic simulations show a shock wave that accelerates as it moves outwards [Fig. 4(c)], which is most easily seen by the temporal increase in energy of the peak in the ion distribution [Fig. 4(d)]. In our simulations, the shock velocity increases by more than twofold during this acceleration period. The mechanism for such shock acceleration is well known and stems from the radially decreasing density profile in the background plasma. In the classic Sedov-Taylor Waxman-Shvarts [26] analysis of the problem, acceleration is seen for steep density gradients. Simple dimensional analysis scaling laws [27], which describe the asymptotic behavior of the shock, are in good agreement with the simulated shock acceleration once we account for the fact that our plasma density is rapidly decreasing with time. Accelerating shock waves are of great interest in astrophysics, and, consequently, experiments have been proposed to investigate such shocks in the laboratory setting [28]. We believe that this study is the first realization of such an experiment and could serve as a versatile platform for studying shocks propagating through customizable density gradients.

Here we demonstrated a new method for studying laser-plasma interactions, which can be implemented using a tabletop apparatus and at a high repetition rate. By characterizing the momentum distribution of individual nanoplasmas, we make the first observation of plasma shock waves on the nanometer scale, confirming a decade of theoretical predictions [4,5,25]. By adjusting the time

delay between two laser pulses, the creation and strength of the shock wave was varied in a controllable manner. Furthermore, because these shocks are produced in plasmas with temperatures of just ~10 eV, this experiment potentially enables a compact, inexpensive method for studying a relatively unexplored regime of low-temperature nanoplasmas.

[1] G. M. Petrov, J. Davis, A. L. Velikovich, P. Kepple, A. Dasgupta, and R. W. Clark, Phys. Plasmas **12**, 063103 (2005).

[2] T. Ditmire, J. Tisch, E. Springate, and M. Mason, Nature (London) **386**, 54 (1997).

[3] T. Ditmire, J. Zweiback, V. P. Yanovsky, T. E. Cowan, and G. Hays, Nature (London) **398**, 489 (1999).

[4] F. Peano, R. A. Fonseca, and L. O. Silva, Phys. Rev. Lett. **94**, 033401 (2005).

[5] A. E. Kaplan, B. Y. Dubetsky, and P. L. Shkolnikov, Phys. Rev. Lett. **91**, 143401 (2003).

[6] F. Peano, R. A. Fonseca, J. L. Martins, and L. O. Silva, Phys. Rev. A **73**, 053202 (2006).

[7] F. Peano, J. L. Martins, R. A. Fonseca, L. O. Silva, G. Coppa, F. Peinetti, and R. Mulas, Phys. Plasmas **14**, 056704 (2007).

[8] T. Ditmire, T. Donnelly, A. M. Rubenchik, R. W. Falcone, and M. D. Perry, Phys. Rev. A **53**, 3379 (1996).

[9] W. Xiong, D. D. Hickstein, K. J. Schnitzenbaumer, J. L. Ellis, B. B. Palm, K. E. Keister, C. Ding, L. Miaja-Avila, G. Dukovic, J. L. Jimenez, M. M. Murnane, and H. C. Kapteyn, Nano Lett. **13**, 2924 (2013).

[10] D. D. Hickstein, P. Ranitovic, S. Witte, X.-M. Tong, Y. Huismans, P. Arpin, X. Zhou, K. E. Keister, C. W. Hogle, B. Zhang, C. Ding, P. Johnsson, N. Toshima, M. J. J. Vrakking, M. M. Murnane, and H. C. Kapteyn, Phys. Rev. Lett. **109**, 073004 (2012).

[11] S. Zherebtsov, T. Fennel, J. Plenge, E. Antonsson, I. Znakovskaya, A. Wirth, O. Herrwerth, F. Süßmann, C. Peltz, I. Ahmad, S. A. Trushin, V. Pervak, S. Karsch, M. J. J. Vrakking, B. Langer, C. Graf, M. I. Stockman, F. Krausz, E. Rühl, and M. F. Kling, Nat. Phys. **7**, 656 (2011).

[12] A. T. J. B. Eppink and D. H. Parker, Rev. Sci. Instrum. **68**, 3477 (1997).

[13] See Supplemental Material at http://link.aps.org/supplemental/10.1103/PhysRevLett.112.115004 for additional details and figures regarding the experiment and simulation.

[14] T. Ditmire, J. W. G. Tisch, E. Springate, M. B. Mason, N. Hay, J. P. Marangos, and M. H. R. Hutchinson, Phys. Rev. Lett. **78**, 2732 (1997).

[15] T. Döppner, T. Fennel, T. Diederich, J. Tiggesbäumker, and K. H. Meiwes-Broer, Phys. Rev. Lett. **94**, 013401 (2005).

[16] T. Döppner, J. P. Müller, A. Przystawik, S. Göde, J. Tiggesbäumker, K.-H. Meiwes-Broer, C. Varin, L. Ramunno, T. Brabec, and T. Fennel, Phys. Rev. Lett. **105**, 053401 (2010).

[17] M. Lezius and S. Dobosz, J. Phys. B **30**, L251 (1997).

[18] T. M. Antonsen, T. Taguchi, A. Gupta, J. Palastro, and H. M. Milchberg, Phys. Plasmas **12**, 056703 (2005).

[19] M. V. Ammosov, N. B. Delone, and V. P. Krainov, Sov. Phys. JETP **64**, 1191 (1986).

[20] J. Dawson and C. Oberman, Phys. Fluids **5**, 517 (1962).

[21] D. S. Gross, M. E. Gälli, P. J. Silva, and K. A. Prather, Anal. Chem. **72**, 416 (2000).

[22] T. Döppner, T. Fennel, P. Radcliffe, J. Tiggesbäumker, and K.-H. Meiwes-Broer, Phys. Rev. A **73**, 031202(R) (2006).

[23] A. Kawabata and R. Kubo, J. Phys. Soc. Jpn. **21**, 1765 (1966).

[24] M. M. Marinak, G. D. Kerbel, N. A. Gentile, O. Jones, D. Munro, S. Pollaine, T. R. Dittrich, and S. W. Haan, Phys. Plasmas **8**, 2275 (2001).

[25] A. Heidenreich, J. Jortner, and I. Last, Proc. Natl. Acad. Sci. U.S.A. **103**, 10589 (2006).

[26] E. Waxman and D. Shvarts, Phys. Fluids A **5**, 1035 (1993).

[27] Y. B. Zel'dovich and Y. P. Raizer, *Physics of Shock Waves and High-Temperature Hydrodynamic Phenomena* (Dover, New York, 2002).

[28] R. Teyssier, D. Ryutov, and B. Remington, Astrophys. J. **127**, 503 (2000).